JOURNAL OF Materials CHEMISTRY

# Synthesis, characterization, photoluminescent and electroluminescent properties of new conjugated 2,2′-(arylenedivinylene)bis-8-substituted quinolines

**Fushun Liang, Jiangshan Chen, Yanxiang Cheng, Lixiang Wang,* Dongge Ma, Xiabin Jing and Fosong Wang**

*State Key Laboratory of Polymer Physics and Chemistry, Changchun Institute of Applied Chemistry, Chinese Academy of Sciences, Changchun 130022, P.R. China.*
*E-mail: lixiang@ciac.jl.cn; Fax: +86-431-5685653; Tel: +86-431-5694787*

***Received 23rd October 2002, Accepted 25th March 2003***
***First published as an Advance Article on the web 8th April 2003***



A series of new PPV oligomers containing 8-substituted quinoline, 2,2′-(arylenedivinylene)bis-8-quinoline derivatives, were designed and synthesized *via* a Knoevenagel condensation reaction of quinaldine, 8-hydroxy- or 8-methoxy-quinaldine with aromatic dialdehydes. These PPV oligomers were characterized by $^{1}H$ and $^{13}C$-NMR, X-ray diffraction, elemental analysis, UV-visible and fluorescence spectroscopies. The X-ray diffraction investigation showed that there are intermolecular π···π interactions in the solid state in **1** and **3**. The optical and photoluminescent properties study demonstrated that the emission color of the resulting materials varies from blue to yellow and is dependent on the substituents (π-donor and π-acceptor groups) on both sides of the conjugated molecules and the aromatic core in the middle of the conjugated backbones. The electroluminescent devices using compounds **1–4** as the emitters and electron-transporting layers were fabricated with the structure ITO/NPB/emitter/LiF/Al. The best device performance with the maximum brightness of 5530 cd $m^{-2}$ and the luminous efficiency of 2.4 cd $A^{-1}$ is achieved by using compound **4**, with intramolecular charge transfer character, as the emitter; these values represent a more than 5-fold improvement in brightness and efficiency compared to compound **3** without methoxy groups on the phenyl rings.

## Introduction

The development of well-defined π-conjugated oligomers has been the subject of intensive research for optoelectronic applications, particularly organic light-emitting devices (LEDs),[1–4] because (i) their precise chemical structure and conjugated length give rise to defined functional properties, (ii) they are able to give high purity films by vacuum deposition,[5,6] (iii) they can serve as model systems for understanding the relationships between bulk material properties and molecular structures in the parent polymers.[7] Recently, interest in the modification of the conjugated backbones by either changing the central cores in the conjugated molecules or changing the electron-donating and/or electron-withdrawing groups to investigate the structural influence on the LED properties was underlined.[8]

The aim of the present work is to develop new poly(phenylenevinylene) (PPV) oligomers containing 8-substituted quinoline for organic light-emitting diodes. The reason for using 8-substituted quinoline as the building block is that both tris(8-hydroxyquinolinato)aluminium ($Alq_3$)[9] and polyquinoline[10] are excellent electroluminescent and electron-transporting materials. In addition, pyridine based conjugated polymers can be used in LEDs made from environmentally stable metal electrodes because of the high electron affinity of the pyridine ring.[11] Therefore, the new class of PPV oligomers containing 8-substituted quinolines is expected to offer the combined properties of PPV and quinolines for organic LED application.

In our previous communication, we reported the synthesis and preliminary light-emitting property of two PPV oligomers containing 8-substituted quinolines.[12] Here, we present the synthesis, structure characterization, electrochemical, photoluminescent and electroluminescent properties of the 2,2′-(arylenedivinylene) bis-8-substituted quinolines (compounds **1–6**) (see Scheme 1 for structures).

## Experimental

### General

$^{1}H$ NMR spectra were recorded on a Varian Spectrometer operating at 400 MHz. Chloroform ($CDCl_3$) and dimethylsulfoxide (DMSO-$d_6$) were used as solvents, and tetramethylsilane (TMS) as internal standard. C, H, N, elemental analyses were conducted with Bio-Rad Co's elemental analytical instrument. UV-vis spectra for compounds **1–6** were obtained from their solutions in chloroform using a Varian Cray 50 spectrometer. A 1 cm quartz cell was used. A typical concentration of $1.5 \times 10^{-5}$ mol $L^{-1}$ was used for the measurements. Photoluminescent spectra were obtained from the same solutions, using a Perkin Elmer LS50B luminescence spectrometer.

### Materials

Standard methods have been used to synthesize 8-methoxyquinaldine[13] and 2,5-dimethoxy-1,4-benzenedicarbaldehyde.[14] 1,4-Benzenedicarbaldehyde, 2,5-thiophenedicarboxaldehyde, isophthalaldehyde, methyl iodide, quinaldine and 8-hydroxyquinaldine (from Aldrich) as well as triethylamine, acetic anhydride (from Beijing Chemical Company) were used without further purification. All reactions were carried out under nitrogen.

**Synthesis of 2,2′-(1,4-phenylenedivinylene)bisquinoline (1).** A mixture of quinaldine (2.68 g, 20 mmol), 1,4-benzenedicarbaldehyde (1.34 g, 10 mmol) and acetic anhydride (10 mL) was stirred and heated at 125 °C for 40 h under $N_2$. It was subsequently poured into ice water (100 mL) and stirred overnight. The brown-green solid obtained was filtered off, washed thoroughly with water, and dried to afford compound **1**. A purified sample (3.26 g, 85%) was obtained as a green solid by recrystallization from a mixture of ethanol and chloroform.

 DOI: 10.1039/b210408c

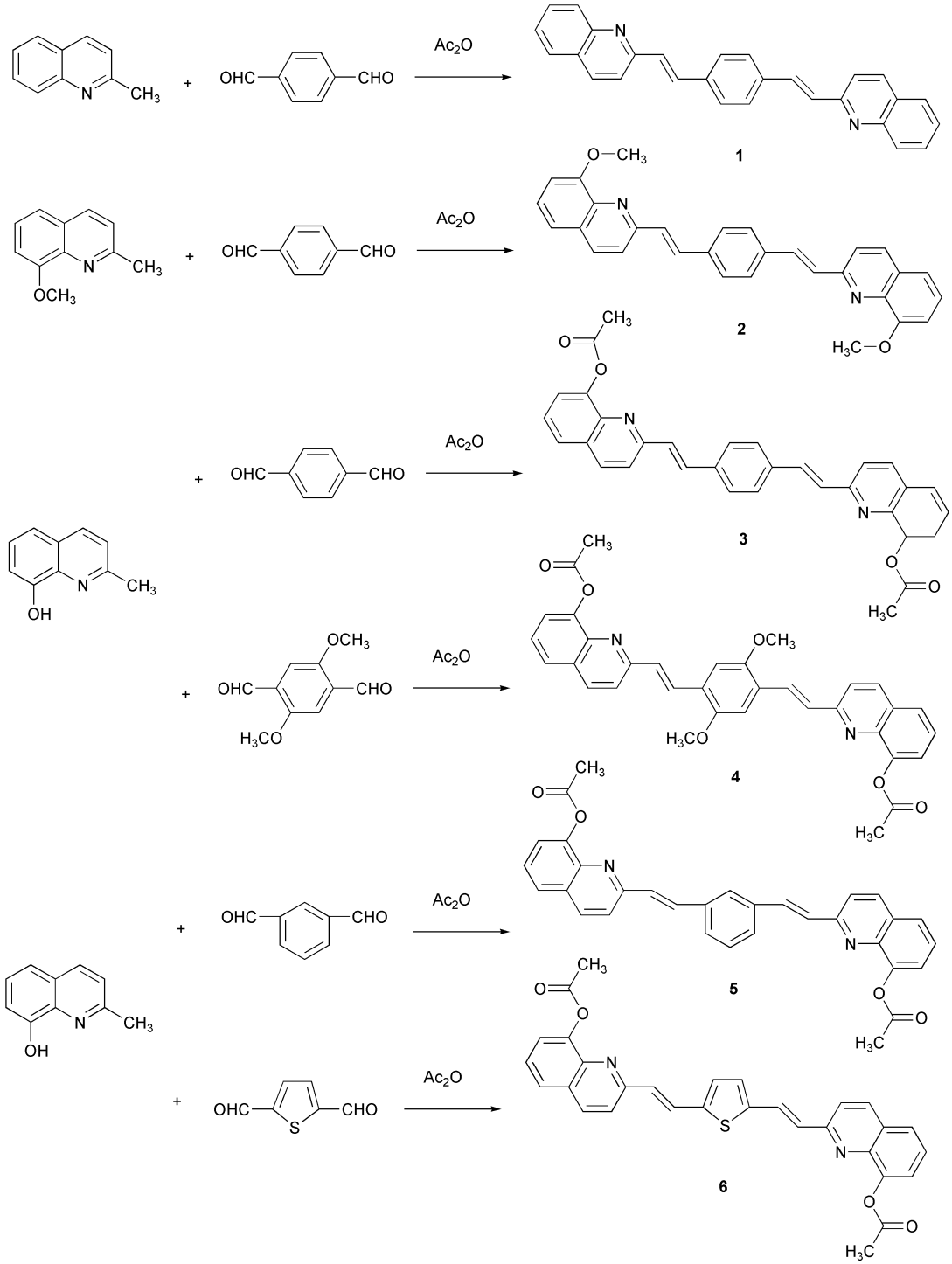


**Scheme 1** The synthetic routes to compounds **1–6**.

M.p. 244–246 °C. $^1$H NMR ($CDCl_3$), $\delta$ [ppm] 7.49 (d, 2H, $J$ = 16.0 Hz, *trans*-olefinic), 7.56 (d, 2H, $J$ = 8.0 Hz, Ar-H), 7.71–7.75 (m, 8H, Ar-H), 7.78 (s, 2H, Ar-H), 7.83 (d, 2H, $J$ = 8.0 Hz, Ar-H), 8.13 (d, 2H, $J$ = 8.4 Hz, 3-position at quinoline), 8.18 (d, 2H, $J$ = 8.4 Hz, 4-position at quinoline). $^{13}$C NMR ($CDCl_3$), $\delta$ [ppm] 119.42, 126.22, 127.39, 127.50, 127.72, 129.25, 129.35, 129.78, 133.81, 136.36, 136.89, 148.33, 155.87. Elemental analysis for $C_{28}H_{20}N_2$, calcd: C, 87.50; H, 5.21; N, 7.29. Found: C, 87.72; H, 5.39; N, 7.52%.

**Synthesis of 2,2′-(1,4-phenylenedivinylene)bis-8-methoxyquinoline (2).** A mixture of 8-methoxyquinaldine (3.46 g, 20 mmol), 1,4-benzenedicarbaldehyde (1.34 g, 10 mmol), and acetic anhydride (10 mL) was stirred and heated at 125 °C for 40 h under $N_2$. It was subsequently poured into ice water (100 mL) and stirred 2 h. After extraction with dichloromethane (3 × 30 mL), the organic layer was washed with water and dried over anhydrous $Na_2SO_4$. The solvent was then evaporated. The resulting residue was purified by chromatography (petroleum ether:ethyl acetate = 2:1 as eluent) to give 2.7 g of product (yield 74%). M.p. 256–258 °C; $^1$H NMR ($CDCl_3$) $\delta$ [ppm] 4.13 (s, 6H, 2 × $OCH_3$), 7.06 (d, 2H, $J$ = 7.6 Hz, 5-position at quinoline), 7.41 (m, 4H, 6,7-position at quinoline), 7.56 (d, 2H, $J$ = 16.4 Hz, olefinic), 7.64 (d, 2H, $J$ = 16.4 Hz, olefinic), 7.66 (s, 4H, Ar-H), 7.77 (d, 2H, $J$ = 8.8 Hz, 3-position at quinoline), 8.12 (d, 2H, $J$ = 8.8 Hz, 4-position at quinoline). $^{13}$C NMR ($CDCl_3$), $\delta$ [ppm] 56.52, 108.36, 119.77, 119.84, 126.81, 127.71, 128.81, 130.92, 133.84, 136.71, 137.23, 140.49, 155.47, 155.58. Elemental analysis for $C_{30}H_{24}N_2O_2$, calcd: C, 81.08; H, 5.41; N, 6.31. Found: C, 81.67; H, 5.61; N, 6.60%.

**Synthesis of 2,2′-(1,4-phenylenedivinylene)bis-8-acetoxyquinoline (3).** A mixture of 8-hydroxyquinaldine (3.18 g, 20 mmol), 1,4-benzenedicarbaldehyde (1.34 g, 10 mmol) and acetic anhydride (10 mL) was stirred and heated at 125 °C for 40 h under $N_2$. It was subsequently poured into ice water (100 mL) and stirred overnight. The brown solid obtained was filtered off, washed thoroughly with water, and dried to afford compound **3**. A purified sample (3.7 g, 82%) was obtained as a yellow solid by recrystalization from DMF. M.p. 252–254 °C. $^1$H NMR ($CDCl_3$), $\delta$ [ppm] 2.59 (s, 6H, $CH_3COO$); 7.40 (d, 2H, $J$ = 16.4 Hz, *trans*-olefinic); 7.43–7.51 (m, 4H, Ar-H); 7.66–7.72 (m, 10H, 8H quinolinol ring except 4-position as well as 2H olefinic); 8.16 (d, 2H, 4-position at quinolinol ring). $^{13}$C NMR ($CDCl_3$), $\delta$ [ppm] 21.42, 120.68, 122.05, 125.93, 126.15, 128.16, 129.01, 129.74, 134.51, 136.74, 137.27, 141.46, 147.84, 156.10, 170.22. Elemental analysis for $C_{32}H_{24}N_2O_4$, calcd: C, 76.80; H, 4.80; N, 5.60. Found: C, 76.93; H, 5.01; N, 5.54%.

**Synthesis of 2,2′-(2,5-dimethoxy-1,4-phenylenedivinylene)bis-8-acetoxyquinoline (4).** A mixture of 8-hydroxyquinaldine (3.18 g, 20 mmol), 2,5-dimethoxy-1,4-benzenedicarbaldehyde (1.94 g, 10 mmol), and acetic anhydride (10 mL) was stirred and heated at 125 °C for 40 h under $N_2$. It was subsequently poured into ice water (100 mL) and stirred for 2 h. After extraction with dicholomethane (3 × 30 mL), the organic layer was washed with water and dried over anhydrous $Na_2SO_4$. The solvent was then evaporated. The resulting residue was purified by chromatography (petroleum ether:ethyl acetate = 2:1 as eluent) to give 2.7 g of product (yield 53%). M.p. 240–242 °C. $^1$H NMR ($CDCl_3$) $\delta$ [ppm] 2.60 (s, 6H, $CH_3COO$), 3.99 (s, 6H, $CH_3O$), 7.29 (s, 2H, Ar-H), 7.39 (d, 2H, $J$ = 16.0 Hz, olefinic), 7.43–7.50 (m, 4H, 6, 7-position at quinoline ring), 7.70 (d, 2H, $J$ = 6.8 Hz, 5-position at quinoline ring), 7.77 (d, 2H, $J$ = 8.8 Hz, 3-position at quinoline ring), 8.12 (d, 2H, $J$ = 16.0 Hz, olefinic), 8.15 (d, 2H, $J$ = 8.4 Hz, 4-position at quinoline ring). $^{13}$C NMR ($CDCl_3$), $\delta$ [ppm] 21.40, 56.74, 109.74, 120.56, 121.99, 125.91, 126.03, 127.24, 128.97, 129.42, 129.70, 136.63, 141.43, 147.81, 152.42, 156.66, 170.34. Elemental analysis for $C_{34}H_{28}N_2O_6$, calcd: C, 72.86; H, 5.00; N, 5.00. Found: C, 73.01.83; H, 5.01; N, 5.28%.

**Synthesis of 2,2′-(1,3-phenylenedivinylene)bis-8-acetoxyquinoline (5).** This compound was prepared by the same procedure as above, but from 8-hydroxyquinaldine and isophthalaldehyde (yield 69%). M.p. 223–225 °C; $^1$H NMR ($CDCl_3$) $\delta$ [ppm] 2.60 (s, 6H, $CH_3COO$), 7.42 (d, 2H, $J$ = 16.4 Hz, olefinic), 7.50 (m, 3H, Ar-H), 7.59 (d, 2H, $J$ = 7.6 Hz, quinoline ring), 7.69–7.75 (m, 6H, quinoline ring), 7.85 (s, 1H, Ar-H), 8.17 (d, 2H, $J$ = 8.8 Hz, 4-position at quinoline). $^{13}$C NMR ($CDCl_3$), $\delta$ [ppm] 21.51, 118.11, 120.06, 122.11, 125.99, 126.47, 127.89, 129.74, 129.96, 134.25, 137.33, 138.42, 147.78, 152.45, 153.79, 156.12, 170.33. Elemental analysis for $C_{32}H_{24}N_2O_4$, calcd: C, 76.80; H, 4.80; N, 5.60. Found: C, 76.91; H, 4.67; N, 5.33%.

**Synthesis of 2,2′-(2,5-thiophenedivinylene)bis-8-acetoxyquinoline (6).** This compound was prepared by the same procedure, but from 8-hydroxyquinaldine and 2,5-thiophenylenedicarboxaldehyde (yield 77%). M.p. 232–234 °C; $^1$H NMR ($CDCl_3$) $\delta$ [ppm] 2.58 (s, 6H, 2 × $CH_3COO$), 7.17 (s, 4H), 7.43–7.50 (m, 4H) 7.56 (d, 2H, $J$ = 9.6 Hz) 7.68 (dd, 2H, $J$ = 8.0 Hz, 1.86 Hz), 7.80 (d, 2H, $J$ = 16.0 Hz, olefinic), 8.14 (d, 2H, $J$ = 8.8 Hz, 4-position at quinoline). $^{13}$C NMR ($CDCl_3$), $\delta$ [ppm] 21.43, 120.84, 122.07, 125.94, 126.08, 127.76, 128.97, 129.27, 129.69, 136.72, 141.47, 143.03, 147.78, 170.21. Elemental analysis for $C_{30}H_{22}N_2O_4S$, calcd: C, 71.15; H, 4.35; N, 5.53. Found: C, 70.86; H, 4.51; N, 5.42%.

## X-Ray crystallography

Crystals of compounds **1** and **3** were obtained from solutions of $CHCl_3$/petroleum ether and were mounted on glass fibers. The data for **1** were collected on a R-AXIS Rapid IP diffractometer, operating at −50 °C, and the data for **3** were collected on a Siemens P4 single-crystal diffractometer with graphite-monochromated Mo K$\alpha$ radiation. The data for compounds **1** and **3** were collected over the 2$\theta$ range of 1.79–27.48° and 2.01–25.01°, respectively. No significant decay was observed for all samples during the data collection. The structure was solved with the direct method of SHELXS-86[15] and refined with full-matrix least-squares techniques using the SHELXL-93 program.[16] All non-hydrogen atoms were refined anisotropically. The crystal of **1** belongs to the triclinic space group $P\bar{1}$, and the crystal of **3** belongs to the monoclinic space group $P2_1/c$. The crystallographic data for compounds **1** and **3** are given in Table 1. Selected bond lengths and angles are given in Table 2. CCDC numbers 195035 (compound **1**) and 170715 (compound **3**). See http://www.rsc.org/suppdata/jm/b2/b210408c/ for crystallographic files in .cif or other electronic format.

## Cyclic voltammetry

Cyclic voltammograms were recorded with a computer controlled EG&G Parc model 273 potentiostat/galvanostat at a constant scan rate of 100 mV $s^{-1}$. Measurements were performed in a conventional three-electrode cell. The working electrode was glassy carbon (diameter 0.8 mm), the counter electrode was a platinum mesh and the reference electrode was Ag/AgCl with a salt bridge containing 0.1 M tetrabutylammonium perchlorate (TBAP) in dichloromethane as the supporting electrolyte. All the experiments were carried out at room temperature and oxygen was removed from all solutions by bubbling nitrogen.

## Fabrication and characterization of the light-emitting devices

The EL devices using **1–4** as the emitting layer were fabricated on an indium tin oxide (ITO) substrate. The ITO glass was routinely cleaned by ultrasonic treatment in detergent solutions, followed by being rinsed with acetone, boiled in isopropanol, rinsed in methanol, and then in de-ionized water. The glass was dried in a vacuum oven between each cleaning step. The electroluminescent device was fabricated by

**Table 1** Crystallographic data of **1** and **3**

| | **1** | **3** |
|---|---|---|
| Formula | $C_{28}H_{20}N_2$ | $C_{32}H_{24}N_2O_4$ |
| $M$ | 384.46 | 500.53 |
| Crystal system | Triclinic | monoclinic |
| Space group | $P\bar{1}$ | $P2_1/c$ |
| $a$/Å | 4.0502(10) | 6.0900(12) |
| $b$/Å | 11.6459(6) | 14.867(3) |
| $c$/Å | 20.9044(11) | 13.880(3) |
| $\alpha$/° | 102.059(10) | 90 |
| $\beta$/° | 90.247(5) | 94.09(3) |
| $\gamma$/° | 91.559(5) | 90 |
| $V$/Å$^3$ | 963.85(7) | 1253.5(4) |
| $Z$ | 2 | 2 |
| $T$/°C | −50 | 21 |
| $\lambda$/Å | 0.71073 | 0.71073 |
| $D_c$/g cm$^{-3}$ | 1.325 | 1.326 |
| $\mu$/cm$^{-1}$ | 0.78 | 0.88 |
| 2$\theta$max/° | 27.48 | 25.01 |
| Data collected | 5649 | 3183 |
| Data unique | 3955 | 2178 |
| Goodness-of-fit on $F^2$ | 1.084 | 0.682 |
| Final $R$ ($I > 2\sigma(I)$) | $R1$ = 0.0541 | $R1$ = 0.0409 |
| | $wR2$ = 0.1584 | $wR2$ = 0.0694 |
| $R$ (all data) | $R1$ = 0.0733 | $R1$ = 0.1350 |
| | $wR2$ = 0.1696 | $wR2$ = 0.0871 |

**Table 2** Selected bond lengths [Å] and angles [deg] for **1** and **3**

| Compound **1** | | | |
|---|---|---|---|
| N(1)–C(9) | 1.309(2) | C(1)–N(1)–C(9) | 117.86(16) |
| N(1)–C(1) | 1.361(2) | N(1)–C(9)–C(8) | 122.96(17) |
| C(1)–C(2) | 1.399(3) | N(1)–C(9)–C(10) | 114.17(16) |
| C(9)–C(10) | 1.468(2) | C(8)–C(9)–C(10) | 122.87(17) |
| C(10)–C(11) | 1.321(3) | C(9)–C(10)–C(11) | 125.52(19) |
| C(11)–C(12) | 1.465(3) | C(10)–C(11)–C(12) | 125.81(19) |
| C(12)–C(13) | 1.396(3) | C(11)–C(12)–C(13) | 123.57(17) |
| C(12)–C(14) | 1.385(3) | C(11)–C(12)–C(14) | 118.41(17) |
| Compound **3** | | | |
| O(1)–C(2) | 1.182(3) | C(10)–N(1)–C(11) | 117.8(3) |
| O(2)–C(2) | 1.374(3) | N(1)–C(10)–C(12) | 117.1(3) |
| N(1)–C(10) | 1.322(3) | N(1)–C(11)–C(3) | 118.7(3) |
| N(1)–C(11) | 1.369(3) | N(1)–C(11)–C(7) | 123.4(3) |
| C(3)–C(4) | 1.356(3) | O(2)–C(3)–C(4) | 120.2(3) |
| C(3)–C(11) | 1.412(3) | O(2)–C(3)–C(11) | 117.1(2) |
| C(10)–C(12) | 1.473(3) | C(4)–C(3)–C(11) | 122.5(3) |
| C(12)–C(13) | 1.333(3) | C(10)–C(12)–C(13) | 123.5(3) |
| C(13)–C(14) | 1.471(3) | C(12)–C(13)–C(14) | 128.7(3) |
| C(14)–C(15) | 1.397(3) | C(13)–C(14)–C(15) | 118.6(3) |

high vacuum ($2 \times 10^{-6}$ Torr) thermal evaporation techniques. A shadow mask with $3 \times 3$ mm$^2$ openings was used to define the cathodes. The EL spectra were recorded with a JY-SPEX CCD-3000 V spectrometer. The current–luminance–voltage characteristics were measured using a Keithley source measurement unit with a calibrated silicon photodiode. All the measurements were performed under atmospheric conditions unsealed.

## Results and discussion

### Syntheses and structures

All the symmetrically disubstituted chromophores were obtained by Knoevenagel condensation reactions. It is well known that the methyl group at the 2-position of the quinoline ring can be activitated by the N atom, then can condense with an aldehyde catalyzed by acid or base.[17,18] In this paper, an acid catalyst was selected. Quinaldine (2 mol) reacted with 1 mol of the appropriate aldehyde, leading to the formation of condensation product **1**. The synthesis of compound **2** was conducted in two stages. First 8-hydroxyquinaldine was reacted with methyl iodide. After separation and purification, the resulting 8-methoxyquinaldine was reacted with 1,4-benzenedicarbaldehyde, affording **2**. For compounds **3–6**, the hydroxy groups were acetylated. The chemical structures of compounds **1–6** were characterized by IR, $^1$H NMR spectroscopy and elemental analysis.

To investigate the intermolecular interactions of the title compounds, their crystal growths were carried out under ambient conditions. Fig. 1 shows the crystal structure and cell packing diagram of compound **1** and Fig. 2 shows the intermolecular hydrogen-bonding interactions in compound **1**. As we can see from Fig. 1 (top), the crystal structure of **1** has an inversion center. Two quinolyl rings in **1** are completely coplanar with the benzene ring, but are on opposite sides of the divinylenebenzylene backbone. Intermolecular π···π stacking and hydrogen-bonding interactions are the most remarkable structural features of compound **1**. A view of the packing of **1** [Fig. 1 (bottom)] shows face to face π···π interactions with the shortest intermolecular π···π interaction distance 3.42 Å between two adjacent molecules. Intermoleular C–H···N hydrogen bonds between the quinoline nitrogen and quinoline hydrogen in compound **1** are observed (Fig. 2). The contact between $C_{21}$–H hydrogen and the quinoline nitrogen atom ($N_1$) of the neighbouring molecule is 2.489 Å. This is clearly within the sum of the van der Waals radii for hydrogen (1.2 Å) and nitrogen (1.55 Å).[19] The $C_{21}$–H···N angle is 163°. These results indicate that the molecules are connected by the extensive array of π···π stacking and hydrogen-bonding interactions.

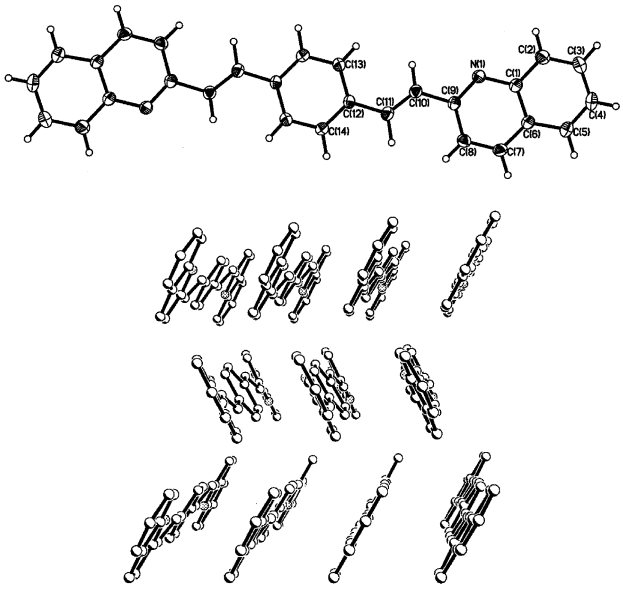


**Fig. 1** Top: one of the independent molecular structure of **1** with labeling schemes and 50% thermal ellipsoids. Bottom: molecular packing diagram of **1** showing the intermolecular π···π interactions.

The crystal structure and cell packing diagram of compound **3** are shown in Fig. 3. Two quinolyl rings in **3** are also coplanar with the benzene ring, on opposite sides of the divinylene-benzylene backbone along with the two acetoxy groups. It can also be seen from Fig. 3 (bottom) that there is extensive stacking between molecules of **3** by π···π interactions in the crystal lattice with the shortest intermolecular π···π interaction distance between two quinolyl rings 3.436 Å.

Munakata *et al.* confirmed that strong intermolecular interactions as well as intermolecular aromatic stacking could assist charge-transfer pathways.[20] The intermolecular π···π interactions suggest that compounds **1** and **3** may possess charge transport abilities, which are essential properties for electroluminescent materials.

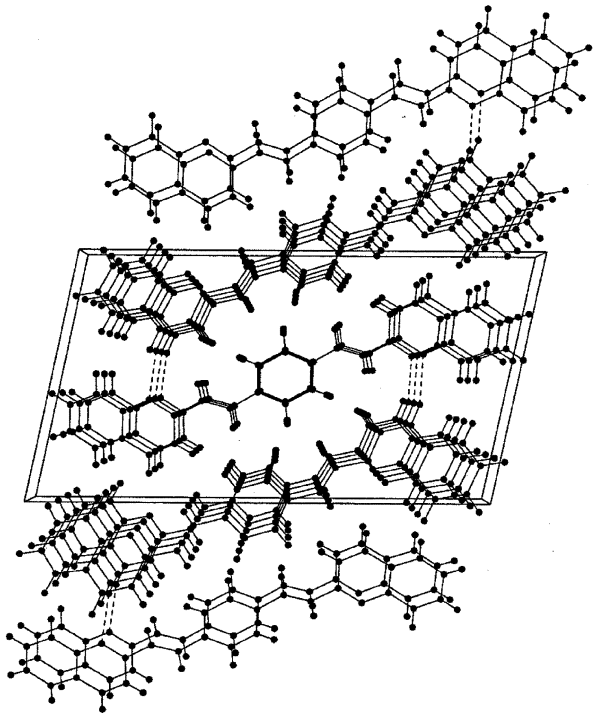

**Fig. 2** Molecular packing diagram of **1** with a view down the *a* axis showing the intermolecular hydrogen-bonding interactions.

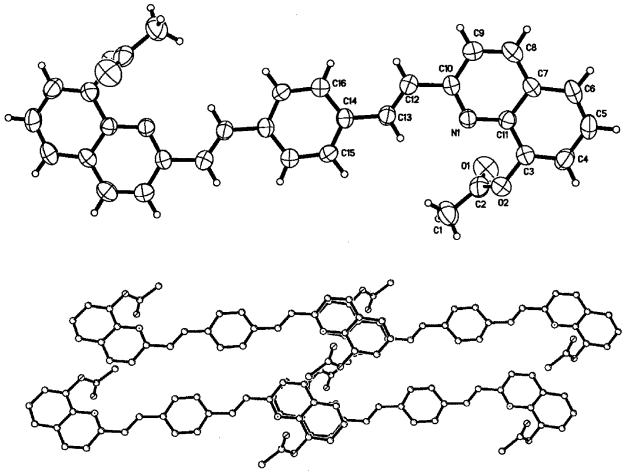


**Fig. 3** Top: the molecular structure of **3** with labeling schemes and 50% thermal ellipsoids. Bottom: unit cell packing diagram of **3**.

## Electrochemical properties

In order to gain information on the charge injection, electrochemical measurements of **1–4** were performed. Typical cyclic voltammetry (CV) curves of compounds **3** and **4** are shown in Fig. 4. The values of onset redox potentials and the HOMO, LUMO energy levels for compounds **1–4** are summarized in Table 3. The energy levels were calculated using the ferrocene (FOC) value of −4.8 eV as the standard and the formal potential of FOC was measured to be 0.12 V against $Ag/Ag^+$.[21] Under a positive scan, irreversible anodic waves was observed for these compounds and the onset potential values located at 1.16–1.39 V, which were higher than that of the model compound, 1,4-bis(4-*tert*-butylstyryl)benzene (1.04 V).[22] Under a negative scan, they showed reductive waves and the onset reduction potentials were between −1.35 and −1.57 V. However, no reduction is observed for model compound 1,4-bis(4-*tert*-butylstyryl)benzene. Obviously this means that introduction of 8-substituted quinoline moieties

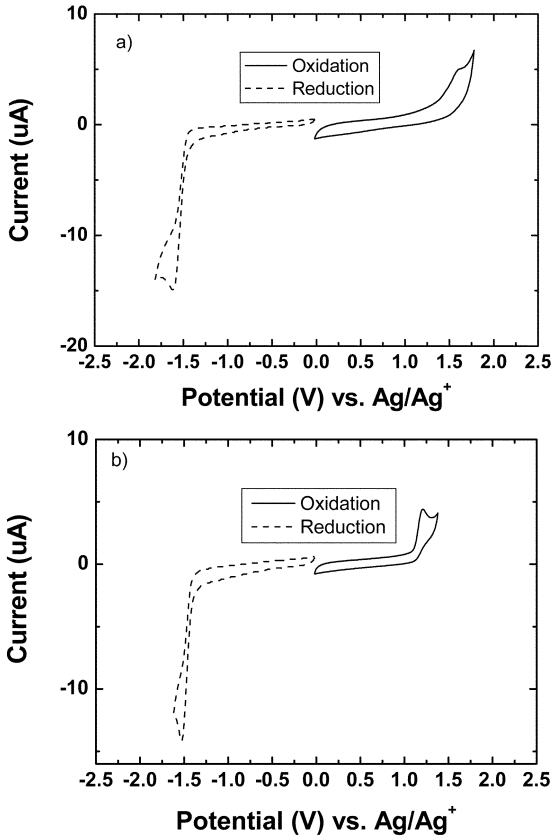


**Fig. 4** Cyclic voltammograms of a) compound **3** and b) compound **4** in 0.1 M $Bu_4NClO_4$ in dichloromethane solution at a scan rate of 100 mV $s^{-1}$.

provides a site of reduction at the unbonded electrons on the nitrogen atom because it is relatively electron deficient. As the reduction process in an electrochemical cell is related to the electron capture ability (or electron injection ability), it was concluded that incorporation of quinoline units onto the OPV backbone enhances the electron affinity significantly, which is beneficial for the construction of highly efficient electroluminescent devices. From the HOMO and LUMO energy levels we can see the low LUMO values (−3.11 to −3.33 eV) will greatly facilitate the electron injection from the cathode of the OLEDs, indicating that an air stable metal such as Al can be chosen as a cathode.

## UV-visible absorption

Absorption spectra for compounds **1–3** in $CHCl_3$ solution are shown in Fig. 5. They exihibited a single structureless and broad absorption peak at 378 nm, which could be assigned to the absorption of the π–π* transition of the conjugated segment. The absorption spectra of **3–6** are shown in Fig. 6, which describes the impact of the variation of aromatic core on the absorption. With *meta*-phenylene instead of *para*-phenylene as an aromatic core in the conjugated backbone, compound **5** possessed a blue-shifted absorption peak at 346 nm, as compared to 378 nm for **3**. It is clear that the incorporation of the *meta*-phenylene linkage provides a means

**Table 3** Redox properties for compounds **1–4**

| Compd. | $E^{ox}/V^a$ | $E^{red}/V^a$ | HOMO/eV$^b$ | LUMO/eV$^b$ |
|---|---|---|---|---|
| **1** | 1.39 | −1.35 | −6.07 | −3.33 |
| **2** | 1.34 | −1.57 | −6.02 | −3.11 |
| **3** | 1.38 | −1.43 | −6.06 | −3.25 |
| **4** | 1.16 | −1.52 | −5.84 | −3.16 |

$^a$Onset potentials *vs.* $Ag/Ag^+$. $^b E_{FOC}$ = 0.12 V *vs.* $Ag/Ag^+$.

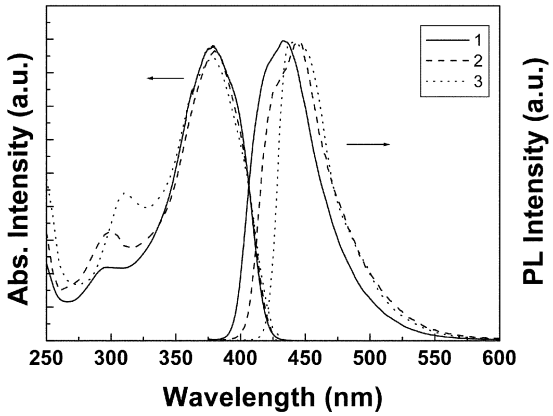


**Fig. 5** UV-vis and photoluminescent spectra of compounds **1–3** in $CHCl_3$ solution. Intensities of absorption spectra have been normalized to the same value. The excitation wavelength of PL spectra is $\lambda_{ex}$ = 365 nm.

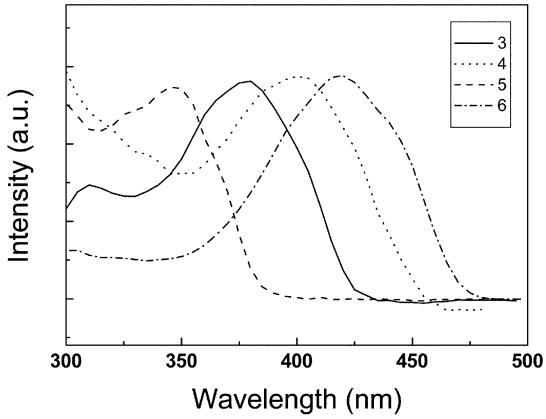


**Fig. 6** Normalized absorption spectra of compounds **3–6** in $CHCl_3$ solution.

to interrupt the π-electron delocalization of the conjugated molecule and then yields a reduction in the effective conjugated length. The replacement of the phenyl ring by a thienyl ring leads to a red shift of the absorption from 378 nm for **3** to 420 nm for **6**. This red-shifting effect mirrors an increase of the conjugated path length in the latter molecule due to the introduction of thiophene unit. It should be noted that a large bathochromic shift (21 nm as compared to compound **3**) occurs by introducing two methoxy groups to the 2,5-position of the central phenyl core. This kind of red shift is also observed in the photoluminescent spectra.

### Photoluminescence

The PL spectra of compounds **1–3** in chloroform solutions, recorded with an excitation wavelength $\lambda_{ex}$ = 365 nm, are listed in Fig. 5. The parent compound **1**, 2,2′-(1,4-phenylenedivinylene)bis-8-quinoline, displays an emission peaked at 435 nm. The methoxy and acetoxy substituted compounds **2** and **3** give maximum emission wavelengths at 443 nm and 439 nm, respectively. These suggest that the bisquinolylvinylenebenzene core is responsible for the blue light emission. Fig. 7 shows the PL spectra of compounds **3–6** in $CHCl_3$ solutions. Compound **3** gives a maximum emission peak centered at 446 nm. Because of the kink of *meta*-phenylene, compound **5** emits blue light with a maximum emission at 429 nm. With the incorporation of the thienyl ring, compound **6** shifts the emission to green (emission peak at 510 nm). Compound **4** shows a green emission with maximum peak located at 481 nm and a shoulder at 506 nm. Compared to **3**, its emission was red-shifted by about 42 nm. This unusual large red shift of compound **4** relative to compound **3** was also observed in its UV-vis absorption. Two possibilities may be considered for the red-shift phenomenon. One is associated with the push–pull effect. It is well known that methoxy is an electron-donor (D) group and the quinolyl ring is an electron-acceptor (A) group. The resulting compound **4** looks like D–π–A structural character and may be involved in the intramolecular charge transfer from the center core to the end groups, which is responsible for the large red-shift.[23–25] Another is merely from the electron-donating effect of the methoxy group, similar to the red-shift of MEH-PPV ($\lambda_{PL}$ = 590 nm ) relative to PPV ($\lambda_{PL}$ = 520 nm).[26,27]

### Electroluminescence of compounds 1–4

To investigate their electroluminescent properties, organic LEDs based on compounds **1–4** as the emitting layer and NPB (*N*,*N*′-di[naphthalenyl]-*N*,*N*′-diphenyl)(1,1′-biphenyl)-4,4′-diamine) as the hole transport layer were constructed because they exhibit intense emissions in both solution and powder states under UV excitation (365 nm). We were unable to examine the electroluminescent properties of compounds **5** and **6** due to their relatively weak emissions in the solid state.

In our experiment, we found that compound **1** was difficult to deposit due to its low volatility. This may be associated with its severe rigidity. After introducing substituent groups at the 8-positions of quinoline rings, compounds **2–4** were easily evaporated during vacuum deposition. It seems that the end substituents were beneficial to reduce the molecular rigidity by free rotation of single bonds. As a result the EL performance of compound **1** was not studied here. Here the detailed device properties of compounds **3** and **4** were presented.

Fig. 8 (top) shows the photoluminescent (PL) spectrum of compound **3** in film state and the electroluminescent (EL) spectrum of structure ITO/NPB (50 nm)/**3** (50 nm)/LiF (1 nm)/Al (200 nm). From the device of compound **3** a bright green light was observed. It was found that the EL spectrum is nearly identical to its PL spectrum in the film state with the maximum emission peak at 518 nm, indicating that the EL emission originates from compound **3**. The current–voltage–luminance (*I*–*V*–*B*) characteristics of double-layer devices using **3** as an emitter are shown in Fig. 8 (bottom). From it one can see that the turn-on voltage was as low as 5 V and the maximum brightness was over 1000 cd $m^{-2}$ at about 18 V. The maximum current efficiency and power efficiency of the device are estimated to be 0.43 cd $A^{-1}$ and 0.13 lm $W^{-1}$, respectively.

The PL spectrum of compound **4** in film state and the corresponding EL spectrum are shown in Fig. 9 (top). Compared with the green light emitting device of compound **3**, this device gave a brighter yellow emission with a maximum emission

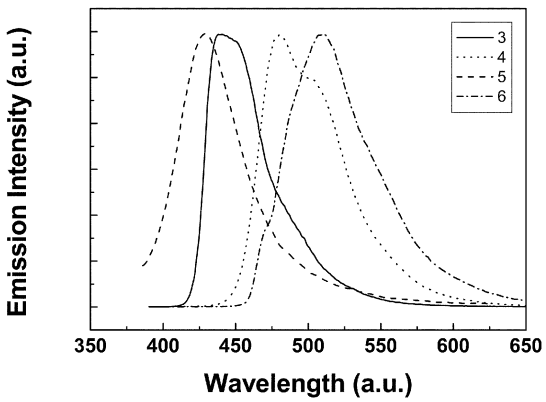


**Fig. 7** Normalized photoluminescent spectra of compounds **3–6** in $CHCl_3$ solution. The excitation wavelength is $\lambda_{ex}$ = 365 nm.

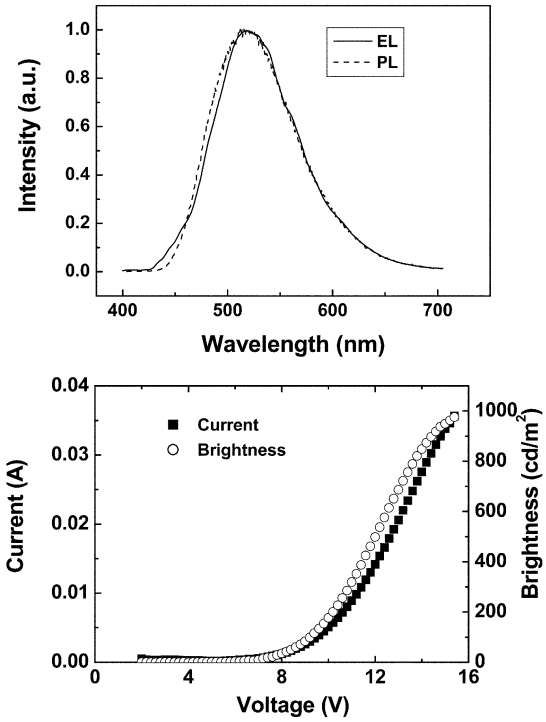


**Fig. 8** Top: PL (film) and EL spectra of **3**. Bottom: the current–voltage–luminance (*I–V–B*) characteristics of double-layer devices using **3** as an emitter.

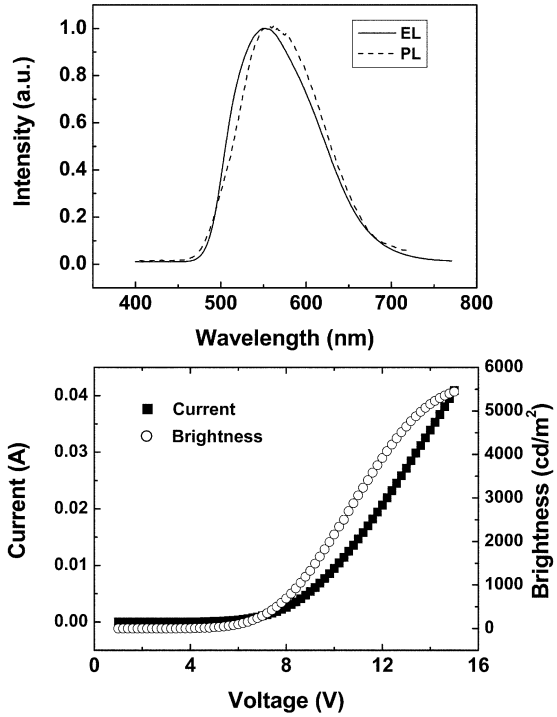


**Fig. 9** Top: PL (film) and EL spectra of **4**. Bottom: the current–voltage–luminance (*I–V–B*) characteristics of double-layer devices using **4** as an emitter.

wavelength of 551 nm. From Fig. 9 (bottom) we can see that the turn-on voltage of this device for compound **4** was only 3 V. The maximum brightness can reach up to 5530 cd $m^{-2}$ at 16 V. The maximum current efficiency of 2.4 cd $A^{-1}$ was obtained at an operating voltage of 7.6 V with a luminance of 500 cd $m^{-2}$, about a 5-fold improvement in brightness and luminous efficiency compared to compound **3** without methoxy groups on the phenyl ring. We believe that the dramatic improvement of the device performance from bisquinoline-containing PPV oligomer **3** to **4** is associated with the difference in chemical structures. This means that when two methoxy groups are introduced into the phenyl ring in the middle of the π-conjugated backbone, the resultant intramolecular charge transfer plays an important role in enhancing the device performance. High EL behavior has been demonstrated in similar molecular systems characteristic of intramolecular charge transfer.[28–30]

## Conclusions

We have developed six new PPV oligomers containing quinoline heterocycles by the simple one-pot Knoevenagel condensation reaction. The resulting PPV oligomers cover the emission region from 435 nm to 510 nm, depending on the substituents (electron-donating and electron-withdrawing groups) on both sides of the conjugated molecules and the aromatic core in the middle of the conjugated backbones. Four of them, compounds **1–4**, have been demonstrated to be promising green/yellow emitters and electron transport materials in organic electroluminescent devices. More important, compound **4** which possesses intramolecular charge transfer character exhibits a significant improvement in double-layer LED performance, with a maximum brightness of 5530 cd $m^{-2}$ and a luminous efficiency of 2.4 cd $A^{-1}$. Further investigation such as device structure optimization is in progress.

## Acknowledgements

This work was supported by the National Natural Science Foundation of China (No. 29725410 and 29992530) and 973 Project (2002CB613402). The authors are also grateful to Professor Wei Xing and Dr. Changpeng Liu for the cyclic voltammetry measurements.

## References

1 F. Hide, M. A. Diaz-Garcia, B. J. Schartz and A. J. Heeger, *Acc. Chem. Res.*, 1997, **30**, 430.
2 S. A. Jenekhe, *Adv. Mater.*, 1995, **7**, 309.
3 A. Kraft, A. C. Grimsdale and A. B. Holmes, *Angew. Chem.*, 1998, **37**, 402.
4 J. L. Brédas, *Science*, 1994, **263**, 487.
5 C. Hosokawa, H. Higashi and T. Kusumoto, *Appl. Phys. Lett.*, 1993, **62**, 3238.
6 C. Adachi, T. Tsutsui and S. Saito, *Appl. Phys. Lett.*, 1990, **56**, 799.
7 T. Maddux, W. Li and L. Yu, *J. Am. Chem. Soc.*, 1997, **119**, 844.
8 H. S. Joshi, R. Jamshidi and Y. Tor, *Angew. Chem., Int. Ed.*, 1999, **38**, 2722.
9 C. W. Tang and S. A. Van Slyke, *Appl. Phys. Lett.*, 1987, **51**, 913.
10 A. K-Y. Jen, X. M. Wu and H. Ma, *Chem. Mater.*, 1998, **10**, 471.
11 M. J. Marsella, D. K. Fu and T. M. Swager, *Adv. Mater.*, 1995, **7**, 145.
12 F. S. Liang, Z. Y. Xie, L. X. Wang, X. B. Jing and F. S. Wang, *Tetrahedron Lett.*, 2002, **43**, 3427.
13 K. Chitoshi, M. Naoyki, K. Noboru, O. Mikio and Y. Akio, *J. Chem. Soc., Perkin Trans. 1*, 2000, **5**, 781.
14 W. Bing and R. Wasielewski, *J. Am. Chem. Soc.*, 1997, **119**, 20.
15 G. M. Sheldrick, *Acta Crystallogr., Sect. A*, 1990, **46**, 467.
16 G. M. Sheldrick, SHELXL-93, Programs for X-Ray Crystal Structure Refinement, University of Göttingen, Göttingen, Germany, 1993.
17 F. Cherioux and P. Audebert, *Chem. Mater.*, 1998, **10**, 1984.
18 A. J. Attias, C. Cavalli, B. Bloch, N. Guillou and C. Noël, *Chem. Mater.*, 1999, **11**, 2057.
19 A. Bondi, *J. Phys. Chem.*, 1964, **68**, 441.
20 M. Munakata, L. P. Wu, T. Kuroda-Sowa, M. Maekawa, Y. Suenaga, G. L. Ning and T. Kojima, *J. Am. Chem. Soc.*, 1998, **120**, 8610.
21 J. Pommerehne, H. Vestweber, W. Guss, R. F. Mahrt, H. Bassler, M. Porsch and J. Daub, *Adv. Mater.*, 1995, **7**, 551.

22 M. S. Liu, X. Z. Jiang, S. Liu, P. Herguth and A. K.-Y. Jen, *Macromolecules*, 2002, **35**, 3532.
23 O-K. Kim, K-S. Lee, H. Y. Woo, K-S. Kim, G. S. He, J. Swiatkiewicz and P. N. Prasad, *Chem. Mater.*, 2000, **12**, 284.
24 M. Albota, D. Beljonne, J-L. Brédas, J. E. Ehrlich, J-Y. Fu, A. A. Heikal, S. E. Hess, T. Kogej, M. D. Levin, S. R. Marder, D. McCord-Maughon, J. W. Perry, H. Röckel, M. Rumi, G. Subramaniam, W. W. Webb, X-L. Wu and C. Xu, *Science*, 1998, **281**, 1653.
25 O-K. Kim and J.-M. Lehn, *Chem. Phys. Lett.*, 1996, **255**, 147.
26 J. H. Burroughes, D. D. C. Bradley, A. R. Brown, R. N. Marks, K. Mackay, R. H. Friend, P. L. Burns and A. B. Holmes, *Nature*, 1990, **347**, 539.
27 A. J. Heeger and D. Braun (UNIAX), WO-B, 92/16023, 1993; *Chem. Abstr.* 1993, **118**, 157401j.
28 L.-H. Chan, H.-C. Yeh and C.-T. Chen, *Adv. Mater.*, 2001, **13**, 1637.
29 X. Q. Lin, B. J. Chen, X. H. Zhang, C. S. Lee, H. L. Kwong and S. T. Lee, *Chem. Mater.*, 2001, **13**, 456.
30 N. Tamoto, C. Adachi and K. Nagai, *Chem. Mater.*, 1997, **9**, 1077.